

Simulating hydroelastic slamming by coupled Lagrangian-FDM and FEM

Martina ANDRUN ^{a,1}, Josip BAŠIĆ ^a, Branko BLAGOJEVIĆ ^a, Branko KLARIN ^a
^a*Department of Mechanical Engineering and Naval Architecture, University of Split*

Abstract. Hydroelastic effects during slamming of high-speed marine vehicles affect the development of the pressure along their bottom. The aim of this study is to investigate coupling process of a novel CFD method and a FEM structural solver for simulation of hydroelastic slamming. As slamming is characterised by violent and strongly nonlinear fluid–structure interaction, the flow solver is based on a Lagrangian, volume–conservative, second–order accurate method, meshless FDM. *Rhoxyz* fluid solver is coupled to *CalculiX* structural solver, through a partitioned bidirectional coupling tool, *preCICE*. After the validation of coupling using a dam break experiment, the effect of hydroelasticity in slamming is studied by analysing the pressure and deformations of the structure during water entries of a deformable symmetrical wedge with low angle of deadrise.

Keywords. Water entry, Slamming, Fluid-structure interaction, Hydroelasticity, Meshless, FDM, FEM

1. Introduction

The problem of slamming or water entry often includes violent and strongly nonlinear fluid-structure interaction (FSI), where such pressures arise that may cause structure deformations and affect ship motions [1]. Mesh-based methods for solving partial differential equations (PDEs) have achieved remarkable success and they have been successfully applied in computational ship hydrodynamics, but creating a topologically correct and geometrically conforming mesh, which needs to be appropriate for the investigated problem, is time-consuming work and often requires user interventions. A simulation that requires large mesh deformations is difficult to maintain in geometrically complex problems, since cautious node movements or re-meshing of deforming areas to avoid mesh tangling and loss of its regularity. On the other hand, overset grid and Lagrangian meshless (or mesh-free) methods have emerged with the goal of avoiding these difficulties encountered in conventional mesh–based methods. Recently a novel meshless Lagrangian method was proposed for numerical simulation of incompressible flows and estimation of hydrodynamic loads during green water events [2]. It was shown that the method accurately reproduces complex free surface patterns, as well as pressure distributions. Furthermore, the fluid is adjusting to moving boundaries represented by triangulated meshes while freely advecting about the boundaries by Lagrangian motion. This property allows the method to directly use structural surface mesh as bounding geometry, and therefore to directly transfer loads between the flow solver and any structural solver. Since the novel flow solver is appropriate for water entry

¹ Corresponding Author, Address: *R. Boskovica 32, 21000 Split, Croatia*; E-mail: *mandru00@fesb.hr*.

problems, and is ready to be coupled to a structural or a rigid-body solver due to the direct use of discrete geometry in fluid simulations, this study deals with establishing a bidirectional fluid-structure interaction (FSI) scheme for slamming. The next few sections describe the fluid solver, structural solver, and their coupling.

2. Flow solver

The method for solving incompressible flows is meshless, Lagrangian, volume-conservative and based on second-order accurate finite differences. Spatial operators are based on generalised finite differences (FDs) in weighted least-squares (WLS) form [3], obtained within the compact sphere of all points shown in Figure 1. Flow is solved using the velocity-pressure decoupled scheme and the volume-conservative Lagrangian advection, obtained by solving a set of geometrical constraints [2]. Due to the fully Lagrangian description of the unsteady fluid flow, the method can handle and simulate violent FSI that includes complex free surface advection with fragmentation. The implementation of the method, named *Rhoxyz* (rhoxyz.com), has been validated for various problems in ship hydrodynamics, including green water [2] and sloshing [4]. The fluid solver works with geometry discretely described by triangles and quadrilaterals, and hence the discrete model of the structure may be directly used in the fluid simulation, which makes the transfer of loads straightforward. The method intrinsically handles violent fluid-structure interaction with free surface fragmentation, while providing second-order accurate pressure field [3]. The detailed information on the method may be found in [2, 3, 4].

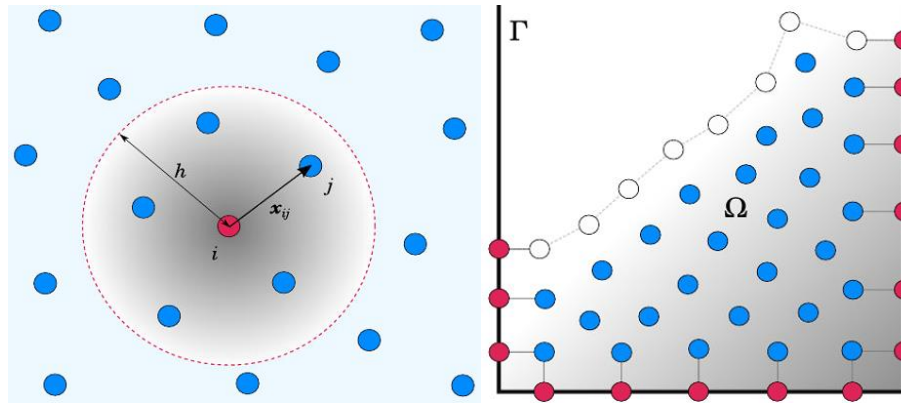


Figure 1. Mesh-free description of fluid (left image), and a domain schematic (right image) that uses no-slip (red) and free-surface (white) boundary conditions.

3. Fluid-structure interaction

In this study, a solver named *CalculiX* [6] is used for structural analysis. It is a validated open-source solver based on the finite element method (FEM). Furthermore, *preCICE* (PREcise Code Interaction Coupling Environment) is an open source coupling tool [7], which is used to set-up partitioned bidirectional coupling of the flow and

structural solvers, *Rhoxyz* and *CalculiX*. As schematically drawn in Figure 2, *preCICE* provides tools for partitioned multi-physics simulation, i.e. iterative methods for solving an interface fixed-point equation, data mapping between non-matching grids, and physical data communication between processes of several solvers. Peer-to-peer communication between solvers allows for massively parallel simulations.

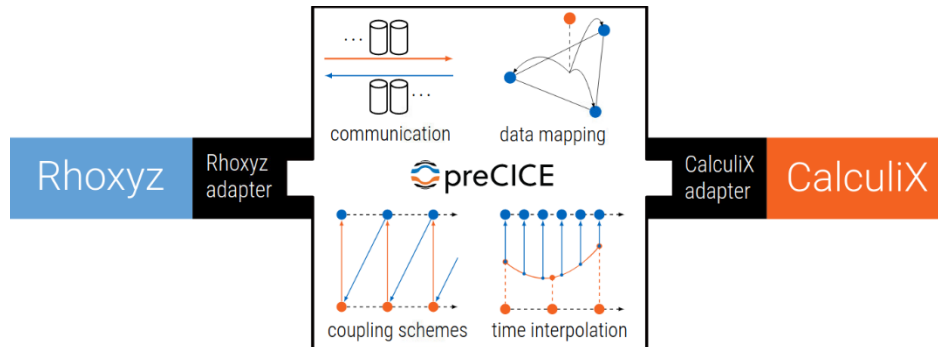


Figure 2. *preCICE* peer-to-peer coupling capabilities (space and time interpolation) are enabled for all participant solvers (in this case *Rhoxyz* and *CalculiX*) through their adapters.

At the start of the time step the solvers synchronise and *preCICE* activates peer-to-peer communication to exchange data between the solvers. This way the fluid solver receives structural deformations, i.e. deflections and velocity vectors of moving nodes. This information is used to impose boundary conditions within the fluid pressure-and-velocity solver. At the same time, the structural solver receives fluid forces acting on each node. It should be noted that even though data mapping between non-matching fluid and structure grids comes at no implementation cost, the same arrangement of nodes was used in this study as the flow solver has the ability to use the same arrangement of structural grid nodes.

The input for *CalculiX* is a single file that describes finite element model using *ABAQUS* notation. In this study, the structure is made of an elastic isotropic material and discretised using eight-node brick elements (C3D8). The only thing needed for coupling from the structural solver-side is to define a set of nodes that are used for two-way transfer of information (e.g. nodes on the bottom of the slamming wedge).

4. Results and discussion

4.1. Slamming validation

In order to validate that method may be used for water entry problems, an experiment from [5] was numerically reproduced. A wedge with 30° of deadrise angle was tilted by 20° about the tip, and then dropped from a height of 500 mm above the free surface. The pressure was measured on the tilted side, 50 mm along the bottom from the wedge tip. The experiment was simulated by rigid-body FSI, i.e. the wedge movement was affected by gravity and fluid forces during the wedge impact. Besides validating the solver for pressures on impact, this experiment proves that the method may be extended for coupling with a more complex structural solver.

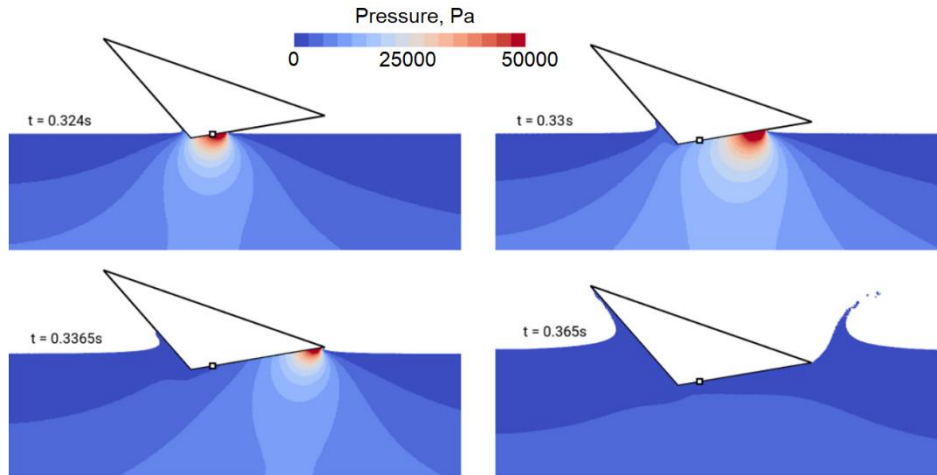


Figure 3. Snapshots of four time-instants of the non-symmetrical water entry with pressure contours.

A series of snapshots of the simulation is shown in Figure 3, which render the movement of the high-pressure area along the wedge during the impact. The pressure gradient area produces a strong jet that detaches from the wedge. The simulated pressure signals shown in Figure 4, for two discretisations with initial point spacings $\Delta = 5$ mm and 2.5 mm, correspond well to the experimentally obtained pressure signal and referent numerical results given in [5]. The pressure field remained stable and smooth at all time, while keeping the flow incompressible.

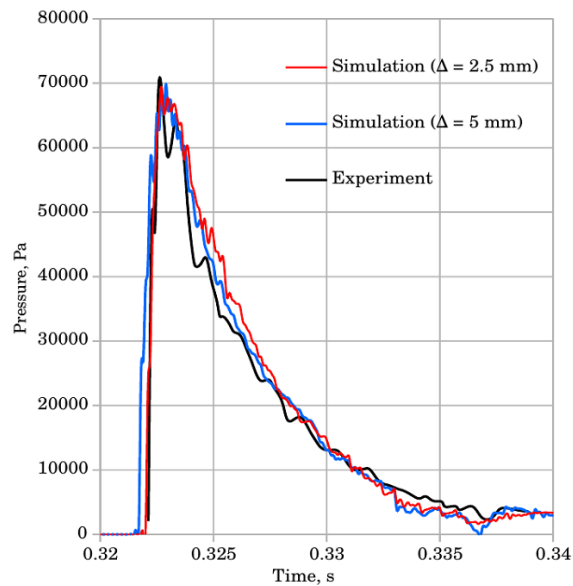


Figure 4. The pressure signal during the impact for the of the non-symmetrical water entry.

4.2. Coupling validation

In order to validate the coupling scheme, an experiment by Kölke [8] was reproduced. The experiment is a typical dam-break problem, in which a water column falls under the influence of gravity and produces a jet that impacts a vertical obstacle on the other end. The elastic obstacle was made of an elastomer with the modulus of elasticity $E = 8 \times 10^6 \text{ g/s}^2/\text{cm}$, the Poisson's ratio $\nu = 0.4$, and the density $\rho = 0.5 \text{ g/cm}^3$. When the wave front hit and deformed the obstacle, it slid along the obstacle and the jet detached from it until impacting the opposite tank wall. The results of the numerical simulation are compared to the experimental images in Figure 5. The structural deformation reached its maximum value before the jet is formed. Afterwards the obstacle swung back to the degree of deformation caused by the hydrostatic pressure on the left side of the obstacle.

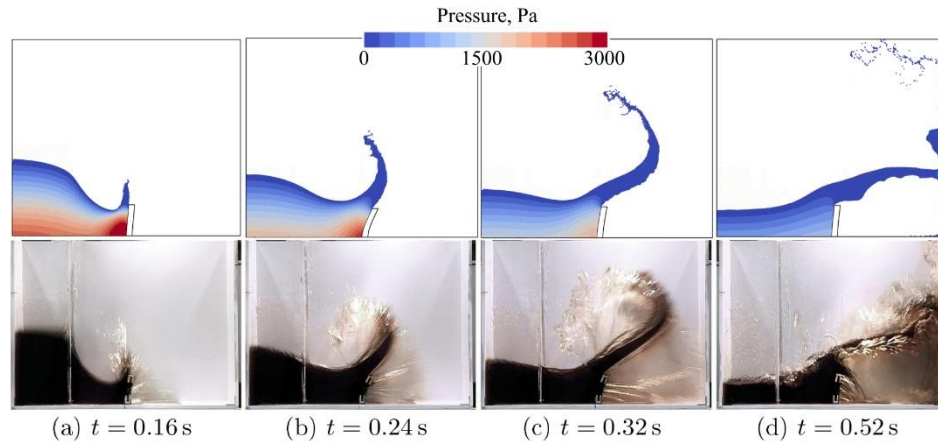


Figure 5. Snapshots of four time-instants of the dam break experiment. Numerical solution is plotted with pressure contours (top row), and the obtained free surface shape and obstacle deformation are compared to the experimental images (bottom row).

4.3. Hydroelastic slamming

In the previous simulated experiment, the structure remained static as water was moving, which resulted in violent FSI. On the other hand, in the water-entry case, the structure is moving while water is static. As the rigid body slamming tests have accurately reproduced pressure fields, and the dam-break tests have accurately reproduced kinematics of the free surface and pressure fields, hydroelastic slamming is investigated. One side of a symmetrical wedge with deadrise of 10° is simulated with constant speed of entry, in order to induce impulsive and moving pressure gradient area. The wedge bottom was discretised using finite elements, while the tip and chine nodes were imposing the fixed boundary condition. The bottom was thick 3 mm, had a beam $B = 500 \text{ mm}$, and entered water with speed $U = 1 \text{ m/s}$. The simulation time step was chosen as constant $dt = 10^{-4} \text{ s}$, while the discretisation spacing was $\Delta = 5 \text{ mm}$.

Firstly, the wedge slamming was simulated as rigid to obtain results for comparison. The second simulation used a flexible model made of Aluminium, with the density of $\rho = 2800 \text{ kg/m}^3$, the modulus of elasticity $E = 70 \text{ GPa}$, and the Poisson's ratio $\nu = 0.33$. In order to analyse the effect of the bottom stiffness on the results, the third simulation was

done after modifying the modulus of elasticity to 7 GPa, and the fourth simulation was done after modifying the modulus of elasticity to 0.7 GPa. Two pressure sensors were placed on the wedge bottom: the first was located at the tip, and the second was located 250 mm from the tip along the bottom.

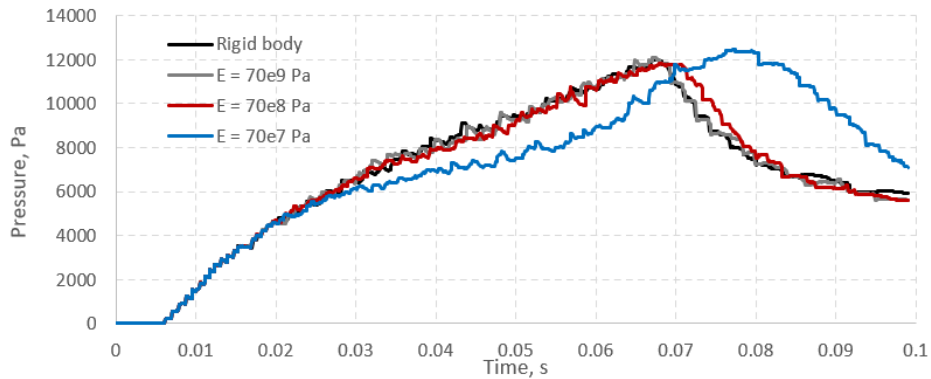


Figure 6. Pressure signal at the wedge tip for four different moduli of elasticity.

The pressure signals recorded by the pressure sensors are presented in Figures 6 and 7. The Aluminium model was stiff for the given entry speed, and it yielded very similar results to the rigid model. By lowering the Young's modulus, the peak of the pressure signal moved forward in time, and the peak magnitude increased. The pressure peak was delayed for flexible models, considering that they generated milder pressure-gradient areas, which moved slower along the bottom. This occurred for the reason that the local angle of deadrise was increasing due to the deformation. In addition to this deformation, the upwards velocity of the deformation generated the suction effect, hence lowering the pressure. Therefore, slope of the pressure signal in Figures 6 and 7 is smaller and smoother for the most flexible model before its sudden increase. Interestingly, the sudden blow-up of the pressure for the most flexible model yielded higher maximum pressures compared to other less flexible models.

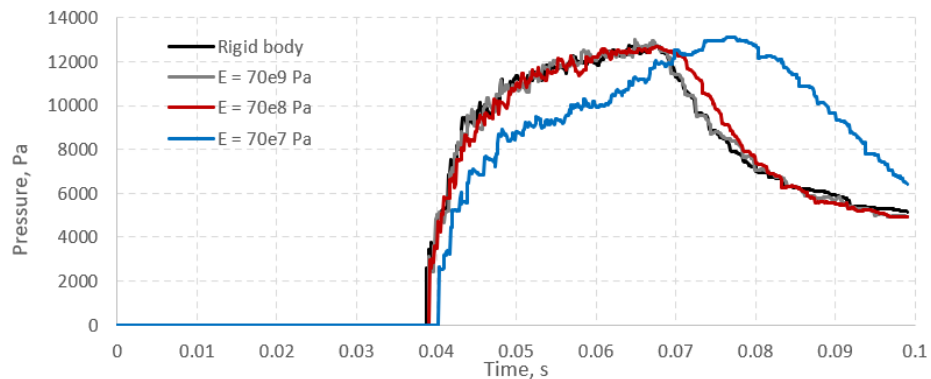


Figure 7. Pressure signal at the wedge tip for four different moduli of elasticity.

Figure 8 renders the simulated pressure field for the rigid and most-flexible models, at two different time instants at which the sensors experience magnitude peaks. Two other simulations are left out from the figure, as their results are very similar to those of the rigid model. 67 ms after the wedge tip reached the free surface, maximum pressure was recorded for the rigid model. As also discussed earlier, it is noticeable that the built-up high-pressure area near the chine moved faster and was stronger along the rigid model. When the high-pressure area slid away from the bottom, high values of the pressure field along the rigid model quickly diminished. Interestingly, this is not the case for the flexible model. As the graphs from Figures 6 and 7 also show, the most flexible model rendered in Figure 8 shows a pressure blow-up, i.e. the high-pressure area moved back from the chine to the wedge tip. 77 ms after the wedge tip reaches free surface, the second sensor for the most flexible model recorded this shock.

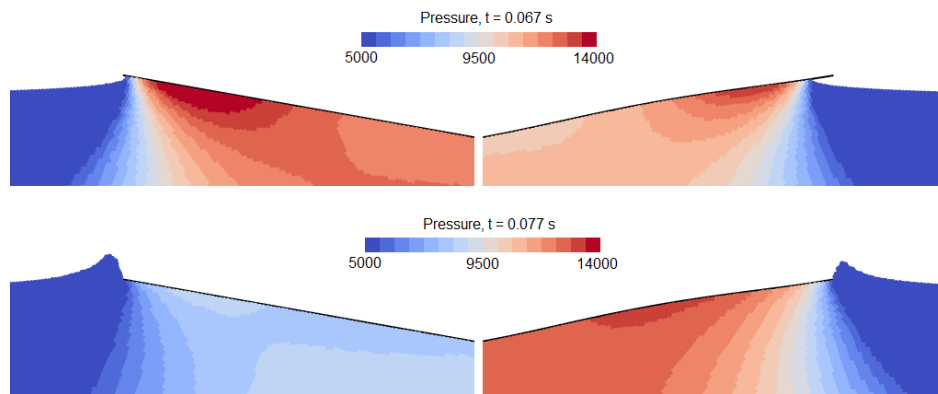


Figure 8. Pressure field around the slamming bottom for rigid model (left column) and the most flexible model (right column).

5. Conclusions

A novel meshless Lagrangian method for the simulation of incompressible fluids with a free surface is applied to rigid-body and hydroelastic slamming problems. Firstly, it was shown that the method accurately simulates rigid-body FSI for an asymmetrical slamming wedge. The method was coupled with a FEM solver using *preCICE*, which facilitated straightforward coupling of the solvers without significant change of the solver algorithms and input files. The coupled scheme was successfully validated on a dam-break problem with a flexible wall, which includes a violent impact of the waterfront. Finally, it was shown that the coupling can handle hydroelastic slamming. Wedges with a low deadrise angle and various stiffness properties were simulated. It was shown that a flexible bottom at constant entry speed may yield larger pressure magnitudes compared to the rigid model. Future work will examine implicit coupling of the solvers for validation of more complex 3D slamming problems.

References

- [1] O. M. Faltinsen, Hydroelastic slamming, *Journal of Marine Science and Technology*, **5** (2000), 49–65.
- [2] J. Bašić, N. Degiuli, Š. Malenica, D. Ban, Lagrangian finite-difference method for predicting green water loadings, *Ocean engineering*, **209** (2020), 107533.
- [3] J. Basic, N. Degiuli, and D. Ban, A class of renormalised meshless Laplacians for boundary value problems. *Journal of Computational Physics*, **354** (2018), 269–287.
- [4] J. Bašić, B. Blagojević, M. Andrun, and N. Degiuli, A Lagrangian Finite Difference Method for Sloshing: Simulations and Comparison with Experiments, *Proceedings of the Twenty-ninth International Ocean and Polar Engineering Conference*, Honolulu, Hawaii, USA, 3412–3418, 2019.
- [5] ISOPE-IHC, Comparative Study on Water Impact Problem for Ship Section & Wedge Drops, *Proceedings of the Twenty-sixth International Ocean and Polar Engineering Conference*, Rhodes, Greece, 2016.
- [6] G. Dhondt, *The Finite Element Method for Three-Dimensional Thermomechanical Applications*. John Wiley & Sons Ltd, Chichester, UK, 2004.
- [7] H. J. Bungartz, F. Lindner, B. Gatzhammer, M. Mehl, K. Scheufele, A. Shukaev, and B. Uekermann. preCICE – A fully parallel library for multi-physics surface coupling. *Computers and Fluids*, **141** (2016) 250–258.
- [8] A. Kölke, *Modellierung und Diskretisierung bewegter Diskontinuitäten in randgekoppelten Mehrfeldsystemen*, Doctoral thesis, Institute of Structural Analysis, TU Braunschweig, 2005.